J. Am. Soc. Mass Spectrom. (2018) 29:1194–1209
DOI: 10.1007/s13361-018-1932-z

FOCUS: MASS SPECTROMETRY IN GLYCOBIOLOGY AND RELATED FIELDS: RESEARCH ARTICLE

Discrimination of Isomers of Released *N*- and *O*-Glycans Using Diagnostic Product Ions in Negative Ion PGC-LC-ESI-MS/MS

Christopher Ashwood,[1,2] Chi-Hung Lin,[1,3,4] Morten Thaysen-Andersen,[1] Nicolle H. Packer[1,2,4]

[1]Department of Molecular Sciences, Macquarie University, Sydney, Australia
[2]Australian Research Council Centre of Excellence for Nanoscale Biophotonics, Macquarie University, Sydney, Australia
[3]Australian Proteome Analysis Facility, Macquarie University, Sydney, Australia
[4]Institute for Glycomics, Griffith University, Southport, Australia

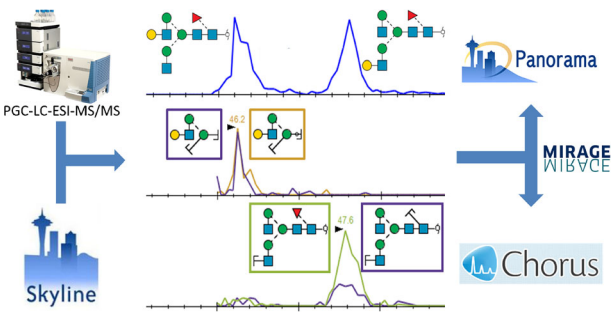

Abstract. Profiling cellular protein glycosylation is challenging due to the presence of highly similar glycan structures that play diverse roles in cellular physiology. As the anomericity and the exact linkage type of a single glycosidic bond can influence glycan function, there is a demand for improved and automated methods to confirm detailed structural features and to discriminate between structurally similar isomers, overcoming a significant bottleneck in the analysis of data generated by glycomics experiments. We used porous graphitized carbon-LC-ESI-MS/MS to separate and detect released *N*- and *O*-glycan isomers from mammalian model glycoproteins using negative mode resonance activation CID-MS/MS. By interrogating similar fragment spectra from closely related glycan isomers that differ only in arm position and sialyl linkage, product fragment ions for discrimination between these features were discovered. Using the Skyline software, at least two diagnostic fragment ions of high specificity were validated for automated discrimination of sialylation and arm position in *N*-glycan structures, and sialylation in *O*-glycan structures, complementing existing structural diagnostic ions. These diagnostic ions were shown to be useful for isomer discrimination using both linear and 3D ion trap mass spectrometers when analyzing complex glycan mixtures from cell lysates. Skyline was found to serve as a useful tool for automated assessment of glycan isomer discrimination. This platform-independent workflow can potentially be extended to automate the characterization and quantitation of other challenging glycan isomers.

Keywords: Glycomics, Diagnostic ions, Skyline, MS/MS

Received: 7 December 2017/Revised: 30 January 2018/Accepted: 1 February 2018/Published Online: 30 March 2018

Introduction

Despite their importance in cell signaling and cell surface biology, glycan structures attached to proteins are frequently avoided as an avenue of investigation, possibly due to their inherent analyte complexity. Glycosylation micro-heterogeneity, the fact that many closely related glycan isomers exist, is an important feature arising from the biosynthesis of glycoproteins and is of proven functional importance, but remains a major analytical challenge in glycomics. The sialyl linkage-type isomers, for example, can influence and define physiology as demonstrated by cancer cells expressing more α2,6- than α2,3-linked sialic acids on glycoproteins, a feature

Electronic supplementary material The online version of this article (https://doi.org/10.1007/s13361-018-1932-z) contains supplementary material, which is available to authorized users.

Correspondence to: Nicolle Packer; *e-mail:* nicki.packer@mq.edu.au

that has been associated with increased metastatic potential [1]. Thus, the ability to accurately, rapidly, and sensitively characterize closely related glycan isomers in a quantitative manner is pivotal to further our understanding of glycobiology.

Mass spectrometry is the gold standard to identify and quantitate the relative abundance of structures in mixtures of glycans released from proteins. The monosaccharide composition and the crude topology of glycans can often be deduced solely from tandem MS data. As glycans are generated through an interconnected biosynthetic pathway, many glycans share common substructures such as core-fucosylation and bisecting *N*-acetylglucosamine (GlcNAc). Diagnostic product ions arising from some of these glycan substructures can be used to confirm topology and link the mass spectral data to structure [2]. Combined with powerful isomer separation using porous graphitized carbon (PGC) LC, which affords an orthogonal identifier by providing informative relative or absolute retention times [3], tandem MS analysis is often able to provide sufficient analyte information for a complete or near-complete structural elucidation of isomers of released glycans, but at very low throughput [4].

The applicability of tandem MS analysis for glycan structure determination and isomer discrimination using negative ion fragmentation has, and continues to be, an area of development with Harvey et al. a leader in this area due to their sizeable contributions [5–11]. While these publications cover a wide range of glycan structures with varying properties that affect their fragmentation mechanisms, there are several key notable trends in the mechanism of diagnostic ions being produced. Typical negative ion fragmentation of glycans involves proton abstraction from various hydroxyl groups throughout the glycan [12]. Through charge-remote and charge-induced fragmentation, abstraction of a proton adjacent to a carbon with an adjacent linkage can result in the generation of cross-ring or glycosidic cleavages, depending on the location of the carbon [13].

Evaluating high mannose [6], hybrid, and complex [7] *N*-glycans, Harvey et al. identified product ions that were specific for 6-arm antenna composition through a commonly shared negative ion fragmentation mechanism. The speculated $C_{R\text{-}1}/Z$ cleavage, diagnostic for extension of the 6-arm, was produced due to charge-remote fragmentation [6]. Analyzing the same glycan structure with positive ion MS/MS, product ions with the same neutral mass can be observed however these ions were produced by an internal cleavage pathway, thus not diagnostic for 6-arm composition [14]. This example demonstrates that the mechanism of how these product ions are produced is important for generating diagnostic ions for glycan isomer discrimination and a suitable fragmentation method is responsible for the ability to reproduce these fragmentation mechanisms for routine glycan analysis.

One technique to generate informative product ions is the use of resonance excitation collision-induced dissociation (RE-CID), commonly utilized in ion trap mass analyzers. RE-CID is attractive due to extremely high fragmentation efficiency and reproducibility, owing to the control of ion populations by ion trap mass analyzers [15]. Combined with negative polarity (−) mode electrospray (ESI)-tandem mass spectrometry (MS/MS), RE-CID serves as an informative dissociation method for determining monosaccharide constituents and glycan topology through production of both glycosidic bond cleavage products (B-/C- and Y-/Z-ions) and cross-ring cleavage products (A-/X-ions) [16].

Despite past studies identifying RE-CID-MS/MS (−) diagnostic ions for specific glycan substructures [6, 17–19], annotation of glycan fragmentation spectra and subsequent determination of glycan substructures remains largely manual. While several software solutions exist for semi-automated glycan spectral annotation from liquid chromatography(LC)-MS/MS-based experiments [20, 21], these software tools are limited to specific glycan analysis workflows, demonstrating the need for universally applicable software.

We utilize Skyline [22], an open source software platform for LC-mass spectrometry(MS) data analysis, to automatically discriminate between highly similar glycan substructures from a complex mixture of glycans released from both purified glycoproteins and proteins from cell lysates, analyzed using negative mode LC-PGC-ESI-MS/MS. In addition, we provide a freely available, detailed workflow for identifying and characterizing new diagnostic ions for their use in isomer discrimination, providing context for their use in an automated analysis platform.

Methods

Materials

All chemicals were sourced from Sigma-Aldrich (Sydney, Australia) unless otherwise specified. Peptide: *N*-glycosidase F (PNGase F, product #: V4831) was obtained from Promega (Sydney, Australia). All solvents used were LC-MS grade and obtained from Merck Millipore (Sydney Australia). Bovine fetuin (product #: F3385) and human IgG (product #: I4506) were sourced from Sigma-Aldrich (Sydney, Australia). All other chemicals were sequencing grade.

Sample Preparation

The J774A.1 cell line (ATCC® TIB-67) was cultured in a T-75 flask with 10 mL of Dulbecco's modified Eagle's medium supplemented with 10% (*v*/*v*) fetal bovine serum. After the adherent cells reached 70% confluency, the growth medium was removed and adherent cells scraped and collected. The cells were washed with phosphate buffered saline, centrifuged (500 g for 10 min) and then the supernatant was removed, for a total of three washes. The cells were then lysed and protein precipitated using a chloroform/methanol/water extraction (10:10:3, by volume). The precipitated protein was removed, re-solubilized in 4 M urea and protein yield quantified with the Bradford protein assay [23].

N- and *O*-glycans were released from the protein samples as described by Jensen et al. [24]. Briefly, 10 μg of the protein

samples were spotted on polyvinylidene difluoride (PVDF) membranes (Millipore, Sydney, Australia) and stained with Direct Blue (Sigma-Aldrich, Sydney, Australia). The membrane spots were excised and washed in separate wells in a flat bottom polypropylene 96-well plate (Corning Incorporated, NY). *N*-Glycans were released from the membrane-bound protein using 1 U PNGase F (Promega, Sydney, Australia) with overnight incubation at 37°C. Following *N*-glycan removal, 500 mM $NaBH_4$ in a 50-mM KOH solution was added to the membrane spots for 16 h to release reduced *O*-linked glycans by reductive β-elimination.

Released *N*-glycans were reduced with 1 M $NaBH_4$ in a 50-mM KOH solution for 3 h at 50°C, after which the reaction was neutralized by adding equimolar glacial acetic acid. Both *N*-glycans and *O*-glycans were desalted and enriched offline using AG 50W-X8 (Bio-Rad) strong cation exchange followed by PGC solid phase extraction micro-columns (Grace, Columbia, MD, USA) prior to analysis.

PGC-LC-ESI-MS/MS Glycan Analysis

PGC-LC-ESI-MS/MS experiments were performed on an UltiMate3000 high-performance liquid chromatography (HPLC) system (Dionex, Sunnyvale, CA, USA) interfaced with a Linear Trap Quadrupole (LTQ) Velos Pro ion trap (Thermo Scientific, San Jose, CA, USA) unless stated otherwise. Some PGC-LC-ESI-MS/MS experiments were also performed on an 3D ion trap using an Agilent 1100 capillary LC system (Agilent Technologies, Santa Clara, CA) interfaced with an Agilent 6330 LC-MSD 3D Trap XCT ultra.

Separations on both instruments were performed using a PGC-LC column (3 μm, 100 mm × 0.18 mm, Hypercarb, Thermo Scientific) maintained at room temperature and at 50°C for the Agilent and Dionex LC systems, respectively. 10 mM ammonium bicarbonate aqueous solution (solvent A) and 10 mM ammonium bicarbonate aqueous solution with 45% acetonitrile (solvent B) were used as mobile phases. The flow rate was 2 and 4 μL/min for the Agilent and Dionex LC systems, respectively. The same gradient was used for both systems with the following linear gradient program: 0 min, 2% B; linear increase up to 35% B for 53 min; linear increase up to 100% B for 20 min; held constant for 5 min; and then equilibrated at 2% B for 5 min before the next injection—giving a total LC run time of 83 min.

MS Parameters

ESI ion source: the ESI-MS^n analysis was operated in negative ion mode with source voltage at - 3.2 kV for both instruments.

For the Thermo Scientific linear ion trap (LTQ), glycans were analyzed according to these MS conditions: *m/z* 580–2000, 3 microscans, *m/z* 0.25 resolution (FWHM), 5×10^4 automatic gain control (AGC) and 50 ms accumulation time and MS/MS conditions: *m/z* 0.35 resolution (FWHM); 2×10^4 AGC, 300 ms accumulation time, 2 *m/z* window and top five data-dependent acquisition. During MS/MS scans, RE-CID fragmentation was used with helium as the collision cell gas. RE-CID subjected ions to 33% normalized collision energy (NCE) with an activation Q of 0.250 and an activation time of 10 milliseconds (ms). For ion trap HCD (Sup Fig. 7), nitrogen was used as the collision gas. HCD subjected ions to 30–37.5% NCE with a default charge state of 2 and an activation time of 2 ms. Spectral data were acquired in profile mode.

For the Agilent 3D ion trap, glycans were analyzed according to these MS conditions: *m/z* 350–2200, 5 microscans, *m/z* 0.13 resolution (FWHM), 8×10^4 ion current control (ICC) and 200 ms accumulation time and MS/MS conditions: *m/z* 0.13 resolution (FWHM), 8×10^4 ICC, 200 ms accumulation time, 4 *m/z* window and top three data-dependent acquisition. RE-CID acquisition, using helium as the collision cell gas, was performed for characterization of the glycan ions detected in MS/MS scans. Fragmentation amplitude was set to 1 V with "Smart Frag" enabled ramping from 30 to 200% of the fragmentation amplitude for RE-CID with an activation time of 40 ms. All spectral data were acquired in profile mode.

Data Availability

In order to adhere to the MIRAGE guidelines [40], complete LC-MS method parameters are listed as Online Resource 3. The raw data files were uploaded to Chorus (Project 1419). Skyline assays were uploaded to Panorama (https://panoramaweb.org/labkey/project/__r3688/begin.view?) and can be inspected. Raw file names and corresponding Skyline assays are listed in Online Resource 4, Supporting Information.

Data Analysis

Manual Identification of Glycans Lists of ions subjected to RE-CID-MS/MS (−) from relevant spectra of each sample were extracted using the ESI-compass v1.3 Bruker Daltonic Software (Bruker DALTONIK GmbH, Bremen, Germany) and RawMeat v2.1 (Vast Scientific, www.vastscientific.com) for the Agilent 3D ion trap and Thermo LTQ, respectively. After removal of common contaminants, the extracted monoisotopic precursor masses potentially corresponding to glycans were searched against GlycoMod (http://www.expasy.ch/tools/glycomod) to identify putative monosaccharide compositions.

Interpretation and validation of glycan identities were based on the existence of A-, B-, C-, X-, Y-, and Z-product ions consistently found across the majority of MS/MS scans over the elution times of the respective precursor ions. GlycoWorkBench v2.1 (available from https://code.google.com/archive/p/glycoworkbench/) was used for most glycan product ion annotation with an in-house monosaccharide product ion database used to cover fragment gaps. Annotated MS2 spectra for all glycan structures can be found in Online Resource 2.

Skyline Settings for Label-Free Glycomics Skyline (64-bit) v3.6.0.10493 (https://skyline.ms/) was used for all analyses at both the MS and MS/MS level.

Settings Used for MS-Level Experiments – Full Scan Settings For the MS-level filtering, isotope peaks were included by count, only filtering for the monoisotopic peak to be used for precursor ion peak area calculation. The precursor mass analyzer was set to a quadrupole ion trap (QIT) with *m/z* 0.5 and *m/z* 0.35 resolution (FWHM) for the Agilent 3D ion trap and the Thermo linear ion trap (LTQ), respectively. High selectivity extraction was used and no retention time filtering was performed. MS/MS filtering was used with acquisition method set to "targeted" with the product mass analyzer set to QIT with *m/z* 0.5 and *m/z* 0.35 resolution (FWHM) for the Agilent 3D ion trap and the Thermo LTQ ion trap, respectively. For Agilent and Thermo QITs, precursor ions were allowed to be in the interval *m/z* 50–2200 as the maximum with a method match tolerance of *m/z* 0.6.

Mass List Preparation for Skyline The precursor ion targets for Skyline analysis were used from a previously developed list of confirmed glycan composition and included information of (1) the glycan class (paucimannose, high mannose, complex, hybrid), (2) confirmed monosaccharide composition/isomer elution order, (3) experimental precursor ion *m/z*, (4) experimental product ion *m/z*, (5) precursor ion charge state, and 6) product ion charge state.

Preparation of Data Files for Skyline Import The Agilent ion trap data files were directly converted to .mzml with Proteowizard (version 3.0.10730, available from *proteowizard.sourceforge.net/* [25]) with no filtering applied, then the .mzml file was imported into Skyline(64-bit v3.7.0.10940) [22]. The Thermo LTQ data files were directly imported to Skyline in their .raw format.

MS/MS-Based Peak Picking in Skyline Identification of glycan isomer discriminators was performed by manual analysis of individual MS/MS scans for each glycan isomer in the standards run on the Thermo LTQ. Product ions were deemed to be discriminators by two criteria: (1) the presence in majority (> 80%) of MS/MS scans for the glycan isomer to be discriminated and (2) detection at greater abundance within the spectrum arising from the targeted glycan isomer compared to all other isomers.

Similar to the MS-level peak picking, the Skyline automatic peak picking algorithm was used but only for manual peak picking of glycans not subjected to MS/MS. The integrated peak areas were exported as per MS-level peak picking. Integrated peak areas were exported using a custom report format made for glycan analysis.

Assessment of Specificity In attempts to reduce the influence of precursor ion intensity in the discriminatory specificity calculations of product ions, product ion intensity was normalized to the intensity of the corresponding precursor ion. We use the definition of specificity as the normalized product ion area for the isomer of interest, divided by the normalized product ion area of all isomers observed.

$$\text{Specificity} = \frac{(\text{isomer of interest product ion area}/\text{isomer of interest precursor area})}{(\text{total product ion area for all isomers}/\text{total precursor area})} \quad (1)$$

Skyline was used for area under the curve integration of precursor and product ions. For isomers of interest, a retention window corresponding to the width of each glycan peak (typical width of 45 s) was selected and peak areas corresponding to the precursor and each product ion were calculated and subsequently exported. For total precursor and product ion areas, multiple retention windows were used corresponding to each isomer present in the samples. Using these retention windows, the area under the curve peak area calculations were performed for the isomers of interest, with the additional step of summing the precursor areas (of the most intense charge state) for each isomer as well as the each product ion area.

Results and Discussion

Observation of Potential Product Ions for Glycan Isomer Discrimination

Negative mode ion trap fragmentation of glycans generates multiple fragment types resulting from glycosidic bond cleavages (B-, C-, Y-, and Z-ion fragments) and cross-ring cleavages (A- and X-ion fragments). This broad spectrum of fragments is useful for differentiating glycan isomers [6, 17].

In Fig. 1, we use these diagnostic product ions to confirm that the *N*-glycan is composed of at least one sialic acid residue (*m/z* 290.09), the antennae sequence is *N*-acetylneuraminic acid (NeuAc)-galactose (Gal)-GlcNAc-mannose (Man) (*m/z* 290.09 (B_1), 470.27 (C_2), 655.29 (B_3), and 817.42 (B_4)) and fucose is attached to the chitobiose core (*m/z* 368.23 ($Y_{1\alpha}$) and 553.31 (Z_2)).

In this case, several structural features could not be determined, including on which glycan arm the antenna is located (i.e., α1,3- or α1,6-mannose arm) and the sialyl linkage (i.e., α2,3- or α2,6-). Determination of these specific structural features is more difficult as it requires not only the presence of the correct product ions but also a manual assessment of the relative product ion intensity [17] and, in some cases, the detection of specific cross-ring fragments and their neutral losses [18].

One typical method for demonstrating the ability of diagnostic fragments to differentiate isomers is by interrogating and comparing the MS/MS spectra of two glycan isomers of the same precursor ion mass. We used this method to identify several product ions which could act as diagnostic ions for bi-antennary *N*-glycan isomers (Fig. 2). As the MS/MS spectra for both glycan isomers was largely similar, subtraction of the

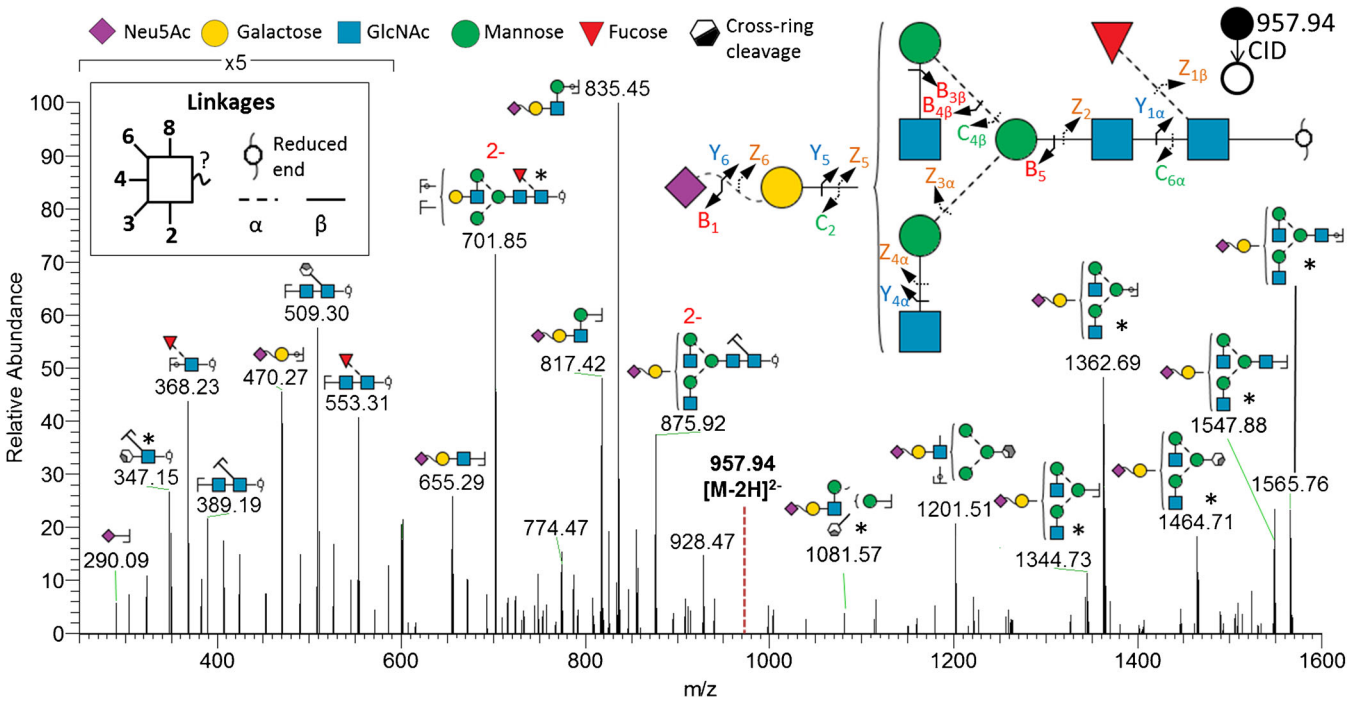

Figure 1. An averaged RE-CID-MS/MS spectrum of a mono-sialylated core-fucosylated bi-antennary complex *N*-glycan. Glycan glycosidic bond cleavages noted in the top right, following Domon and Costello nomenclature. Sialic acid linkage and arm composition could not be determined using the ions acquired. Asterisk (*) denotes structures with more than one possible isomer, only one possible structure per product ion annotated for clarity

spectra was performed to identify ions that are present at greater intensity in one spectrum compared to the other. As a result of this MS/MS spectrum subtraction process of *m/z* 812.37 $[M\text{-}2H]^{2-}$ isomers, we identified *m/z* 304.08 ($B_{2\alpha}{}^{0,4}X_{1\alpha}$), 1260.72($Y_{4\alpha}$), 1281.72 ($Z_{5\alpha}Z_{1\beta}$), and 1445.76 ($Z_{5\alpha}$) as being more abundant in the fragment spectrum for isomer B which possesses a galactosyl extension of the α1,3-linked mannose arm of the bi-antennary *N*-glycan. This structure was also orthogonally confirmed by the PGC elution order [3] with the galactosyl extension of the α1,6-linked mannose arm resulting in an earlier elution compared to an *N*-glycan structure with a galactosyl extension of the α1,3-linked mannose arm. One limitation in the subtraction process is the observation of more intense isotopic peaks for more abundant isomers, which do not correspond to monoisotopic peaks of glycan fragments. To address this limitation, we confirmed these product ions to be monoisotopic peaks through visual examination of the mass spectra and utilization of GlycoWorkBench as an in silico approach to confirm each product ion as a theoretically possible glycan fragment. While this process identified candidate product ions for glycan isomer discrimination, the characterization of product ion abundance and specificity and their relationship with collision energy is important to determine their usefulness as diagnostic ions.

Optimization and Validation of Product Ions that Discriminate Glycan Isomers

As glycans can vary in size, structure, and net charge, which may affect dissociation pathways and therefore the ability to discriminate glycan isomers, optimization of collision energy was performed with several glycan structures of interest (Fig. 3). These glycan structures were chosen as they are typically abundant in *O*- and *N*-linked releases of glycans from mammalian glycoprotein mixtures and cover a wide range of masses (676–2225 Da) and are both asialo- and sialoglycans, which contribute to charge localization and therefore fragmentation pattern [5]. Evaluating first the degree of precursor dissociation, we observed that 28% normalized collision energy (NCE) was the lowest energy required to completely fragment all glycan precursors except for the *O*-glycan (*m/z* 675 $[M\text{-}H]^{1-}$) but the second lowest collision energy assessed, 33% NCE, was effective for complete dissociation of all structures. This could be explained by, following conversion equations to determine the amount of energy applied from NCE% [26], the *m/z* 675.30 ion being subjected to the lowest amount of energy compared to energy used for the heavier ions (Supp. Table 1).

Regarding discriminator abundance, no one collision energy value generated the most intense glycan fragments for all glycan structures. The 48% NCE setting generated on average the lowest amount of product ions. This may be the result of resonant ejection of precursor ions with higher fragmentation energies which has been found by Webb et al. [27].

For the glycan corresponding to *m/z* 675.30 $[M\text{-}H]^{1-}$, discriminator abundance levels were strongly linked to the total product ion intensity, rather than the amount of energy applied. For the glycan corresponding to *m/z* 812.37 $[M\text{-}2H]^{2-}$, varying collision energies changed the relative abundance of several product ions for each discriminator (e.g., discriminator 3 had a relatively low

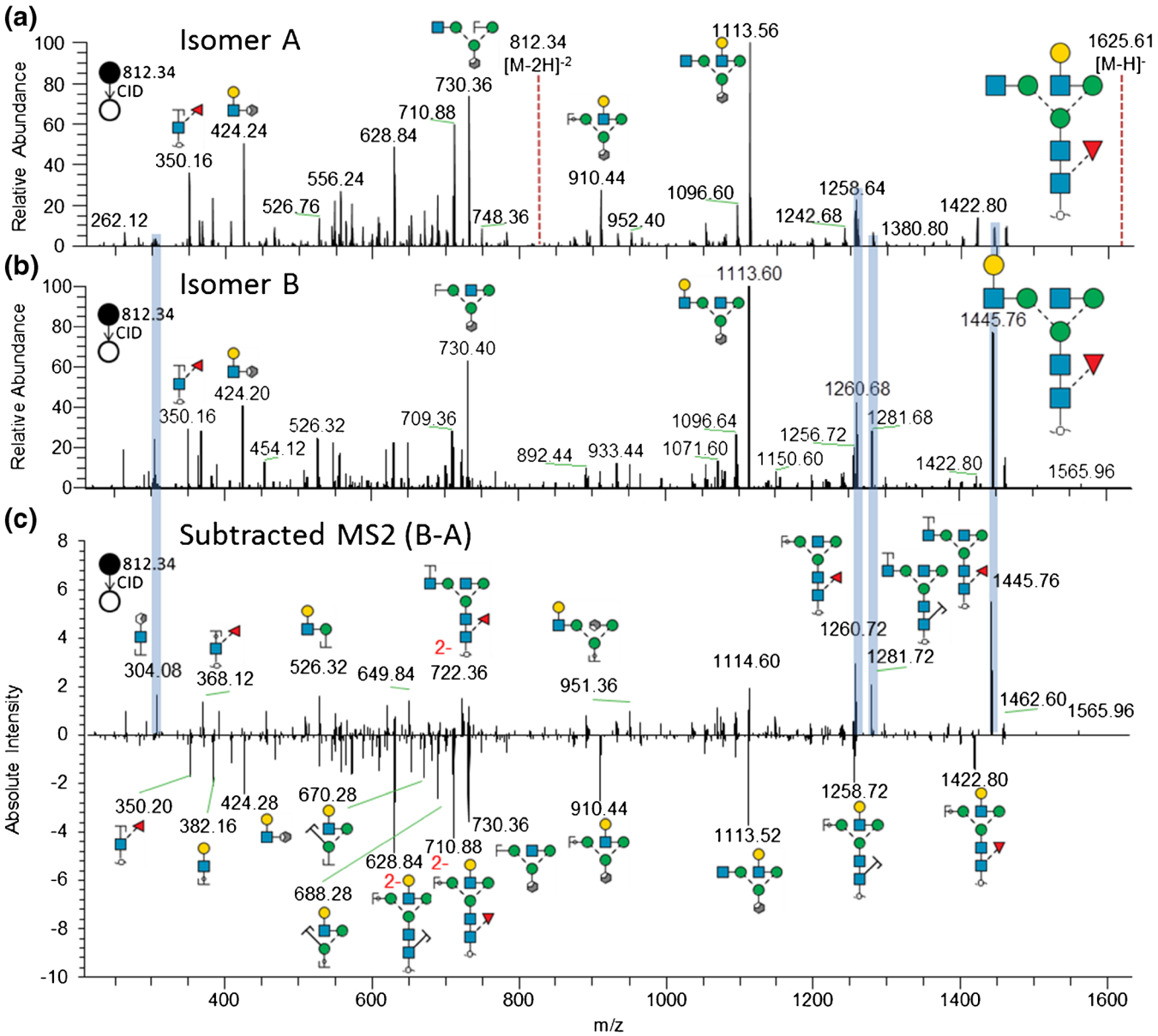

Figure 2. Identification of discriminatory candidate product ions for two neutral *N*-glycan isomers (*m/z* 812.34 $[M\text{-}2H]^{2-}$). (**a**) Average RE-CID-MS/MS spectra for (**a**) isomer A, (**b**) isomer B, and (**c**) isomer B subtracted by isomer A. Only one possible fragment per product ion is annotated for clarity

abundance at 38% NCE compared to other assessed collision energies). As a result of this optimization, we chose 33% NCE as the optimal collision energy for complete fragmentation of the precursor ions while producing the most intense product ions.

Discrimination of N-Glycan Arm Extension by Specific Fragment Ions

Previous publications identifying product ions useful for distinguishing glycan isomers often do not feature a quantitative assessment of how specific the chosen product ions are for the isomer that they represent. This hinders the application of these diagnostic ions. We utilize an equation (Eq. 1 above) to give a semi-quantitative assessment of the specificity of the putative discriminatory product ions. In attempts to reduce the influence of precursor intensity on the specificity calculations of product ions, product ion intensity was normalized by the corresponding precursor ion intensity. We use the definition of specificity as the normalized product ion area for the isomer of interest, divided by the normalized product ion area of all isomers observed.

As seen in Fig. 4, we have used published diagnostic ions for core-fucose (*m/z* 350.20 ($Z_{1\alpha}$) and 368.16 ($Y_{1\alpha}$)) and 6-arm composition (*m/z* 670.28 ($B_4Z_{3\alpha}$) and 688.32 ($B_4Y_{3\alpha}$) at 95 and 97% specificity, respectively) to confirm core-fucosylation on both *N*-glycan isomers and identify the glycan structure with 6-arm galactosyl extension, respectively [28, 29]. To identify the other glycan isomer featuring a 3-

Table 1. List of Glycan Fragments for Isomer Discrimination Used for Fragmentation Optimization in Fig. 3 and Their Respective Glycan Structure Fragments (in Cases Where Isomers Exist for a Given Fragment, Only One Structure Is Shown)

Precursor *m/z* (Isomer)	Discriminator			Precursor *m/z* (Isomer)	Discriminator		
	#	Product *m/z*	Probable fragment		#	Product *m/z*	Probable fragment
675.30 (B)	1	384.20 $[M-H]^{1-}$	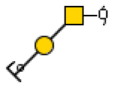	812.37 (A)	1	1258.72 $[M-H]^{1-}$	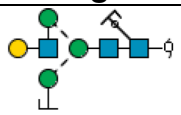
	2	631.32 $[M-H]^{1-}$	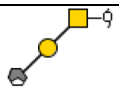		2	571.32 $[M-H]^{1-}$	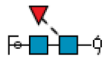
	3	204.08 $[M-H]^{1-}$			3	670.28 $[M-H]^{1-}$	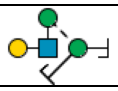
	4	380.16 $[M-H]^{1-}$			4	910.44 $[M-H]^{1-}$	
	5	222.08 $[M-H]^{1-}$			5	688.32 $[M-H]^{1-}$	
965.96 (A)	1	835.40 $[M-H]^{1-}$		1111.58 (A)	1	1000.6 $[M-2H]^{2-}$	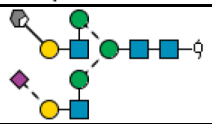
	2	817.40 $[M-H]^{1-}$			2	1002.00 $[M-2H]^{2-}$	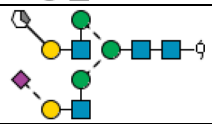
	3	655.36 $[M-H]^{1-}$	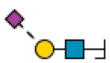		3	889.4 $[M-2H]^{2-}$	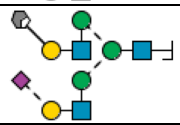
	4	701.84 $[M-2H]^{2-}$	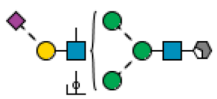		4	898.92 $[M-2H]^{2-}$	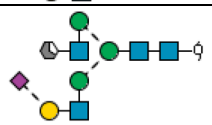
	5	1387.64 $[M-H]^{1-}$	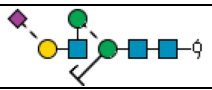		5	891.48 $[M-H]^{1-}$	

arm galactose residue, we have observed glycosidic cleavage product ions specific for this isomer (*m/z* 1445.76 ($Z_{5\alpha}$), 1281.72 ($Z_{5\alpha}Z_{1\beta}$) at 91 and 80% specificity, respectively). The specificities of the product ions for 3-arm position were slightly lower than those routinely used for determination of 6-arm position [29] showing that our shotgun glycomics method is compatible with previously published diagnostic product ions for determining glycan structural features. These previously published diagnostic ions were first detected on a Q-ToF platform using beam-type CID highlighting that this workflow can use diagnostic ions resulting from alternative fragmentation methods and mass analyzers. Through our characterization of the specificity of these diagnostic ions on our platform, we have provided parameters for their use in both manual and automated analysis. These proposed diagnostic ions are of similar intensity and specificity, making them useful in routine analyses.

Interestingly, both structures share core-fucose diagnostic ions but these ions are not represented equally in the MS/MS spectra of both isomers, with the *m/z* 350.20 and *m/z* 368.16 product ions being 70 and 36% specific for the same isomer, respectively. The difference between these two product ions is their type of cleavage with the *m/z* 350.20 ion being a Z_1 cleavage product (cleavage by H^- transfer following deprotonation) whereas the *m/z* 368.16 ion is a Y_1 cleavage product (cleavage by deprotonation) [16]. These results suggest that slight changes in arm composition at the non-reducing end of the glycan affect the production of specific glycan cleavage products at the reducing end which theoretically can provide

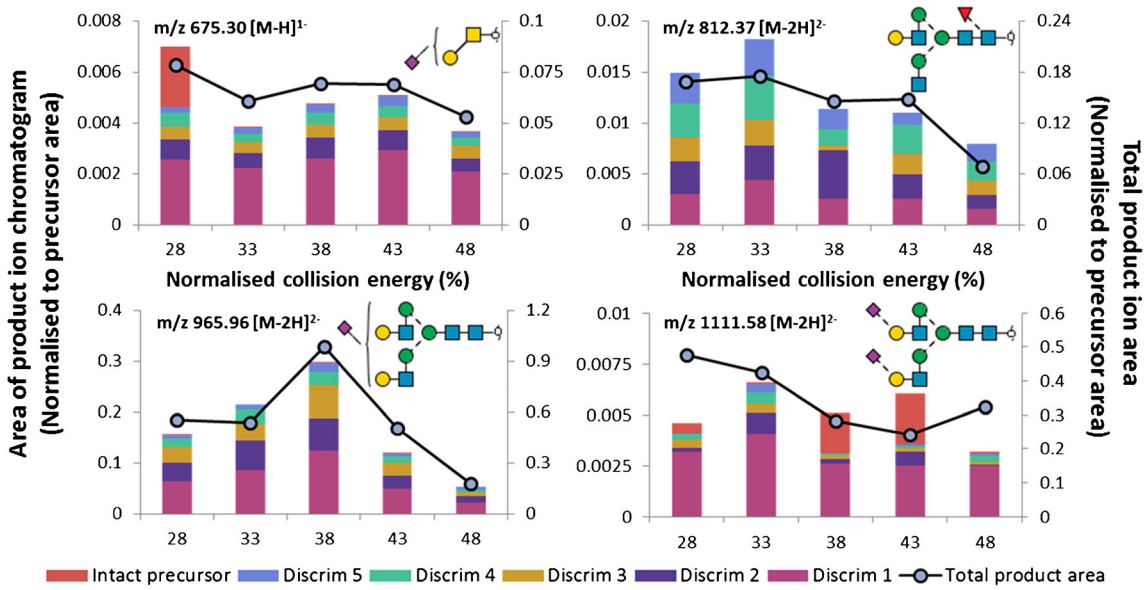

Figure 3. Optimization of CID energy for different *O*- and *N*-glycan structures. Discrimination candidates (detailed in Table 1) and unfragmented precursor ion peak areas assessed as well as total product ion area. All values normalized by precursor peak area. Glycan structures confirmed with MS/MS analysis and sialidase treatment (Supp. Figs. 2 and 3). Raw data can be found in Online Resource 1

candidates for discrimination between isomers with only non-reducing end structural differences.

All product ions assessed were of similar intensity, suggesting these newly identified discriminators for 6-arm position are likely to be observed in any MS/MS spectra where core-fucosylation could be confirmed, therefore not requiring additional accumulation time or increased number of ions for additional structural characterization. As a result of the identification of the 3-arm diagnostic fragments, we can combine these fragments with previously identified 6-arm diagnostic fragments to automatically discriminate and quantitate, by integration of the area under the curve, these glycan isomers in complex mixtures.

Discrimination of Sialyl Linkages by Specific Fragment Ions: N-Glycans

Terminal anionic sialic acids are of great importance in cancer biology. Determination of sialic acid linkages remains an analytical challenge. As shown in Fig. 5, using the candidate MS/MS diagnostic ions for α2,6 sialic acid linkage (*m/z* 835.40 (C_4), 817.40 (B_4), 655.36 (B_3)) and α2,3 sialic acid linkage (*m/z* 979.44 ($B_5Y_{4\alpha}$), 1276.72 ($Y_{6\beta}Y_{4\alpha}$), 1506.80(B_5)), we have identified glycosidic cleavage product ions specific for either α2,6- and α2,3-sialic acid linkages with at least two product ions (*m/z* 817.40/835.40 and *m/z* 979.44/1276.92) having greater than 80% specificity. This specificity value was a goal as it theoretically would be able to correctly discriminate glycan isomers when the glycan isomer of interest is 20% of the peak area of the other isomer, reducing the amount of manual intervention required for integration of glycan isomers.

When evaluating the type of fragments that are specific for each sialic acid linkage, the α2,6-sialoglycan diagnostic fragments are B- and C-type fragments of the antennae whereas the α2,3-linked sialic acid diagnostic fragments are CY-, YY-, and B-type fragments. It can then be hypothesized that changing the sialic acid linkage has an observable effect on the fragmentation pathway that the glycan structure undergoes, thus resulting in differently favored cleavage types that allow discrimination of the two isomeric structures. Charge state of the precursor also can influence the dissociation pathway; however, we have only studied the most abundant charge state as it would be selected more frequently in a data-dependent MS experiment [30].

Previously published sialyl linkage discriminators have been reported to determine the presence of α2,3- or α2,6-linked sialic acid through cross-ring cleavages and neutral losses [18]; however, these ions were either not detected or found to be specifically generated by our analytical platform. As shown in Figs. 1 and 2, the abundance of cross-ring fragments is qualitatively different compared to previously published glycan structure MS/MS spectra [7, 8, 29]. One notable difference is the inability to produce a $^{2,4}A_R$ ion, as described by Harvey et al. notation [11], due to the open-ring reduced GlcNAc making cyclic electron shift unable to occur. In addition to the difference in cross-ring product ions, we have increased intensity of C-type fragments, which have been observed by Harvey to decompose into cross-ring fragments with their beam-type CID platform [6]. We speculate we have reduced the decomposition rate from C-type fragments into cross-ring fragments due to the lower activation energy used in our RE-CID method compared to beam-type CID [3].

Overall, we have found it difficult to pinpoint an exact cause for the slight difference in our MS/MS spectra to

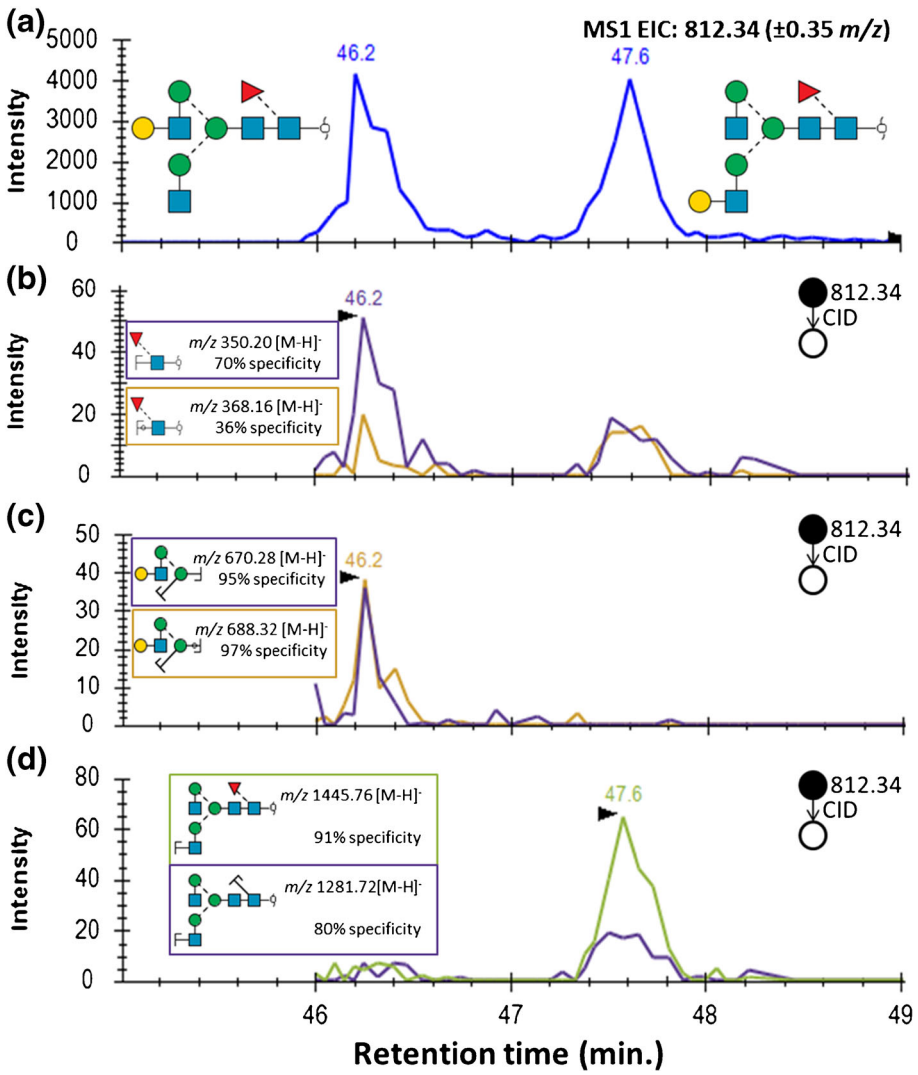

Figure 4. Automated core-fucosylated bi-antennary mono-galactosylated *N*-glycan isomer discrimination using validated and candidate product ions. EICs of (**a**) the glycan precursor (*m/z* 812.34 $[M\text{-}2H]^{2-}$ $(Man)_3(Gal)_1(GlcNAc)_4(Fuc)_1$), (**b**) diagnostic product ions showing core-fucosylation, (**c**) validated diagnostic product ions for 6-arm composition, and (**d**) previously unreported diagnostic ions for 3-arm composition

published spectra by Harvey et al. due to a number of differences between CID methods. For example, between Harvey et al. [29] and the experimental method presented our study, all the MS parameters (except negative polarity) that affect fragmentation differ: collision gas (we used nitrogen, Harvey et al. used argon), CID mechanism (we used resonant excitation, Harvey et al. used beam-type) and activation energy (we used low energy, mV, while Harvey et al. used high energy, V).

By our use of the identified glycosidic bond diagnostic ions generated by RE-CID, we show that we can discriminate sialic acid linkage isomers of *N*-glycans. Similar to the diagnostic product ions we identified for discriminating the 3- and 6-arm mannose antenna extension, the product ions used for discriminating sialic acid linkages are abundant thereby allowing their use for automatic discrimination in a typical shotgun glycomics experiment.

Compared to the mono-sialylated *N*-glycan isomers, bi-sialylated *N*-glycans are more difficult to identify with discriminatory ions because there are four possible sialic acid linkage combinations (α2,3/α2,3-, α2,3/α2,6-, α2,6/α2,3-, and α2,6/α2,6-) as opposed to mono-sialylated *N*-glycans with only two possible linkage combinations (α2,3- or α2,6-). As demonstrated in Fig. 6, using the candidate diagnostic ions for α2,6/α2,6-sialic acid linkage (*m/z* 898.92 ($^{1,5}X_6$)/891.48 ($^{3,5}A_5$) and α2,3/α2,3 sialic acid linkage (*m/z* 1375.76 ($^{2,5}X_6Y_6$)/1295.60 ($^{1,4}A_7Z_3$)), we have identified cross-ring cleavage product ions specific (> 95%) for bi-sialylated *N*-glycans with homogeneous sialic acid linkages. Diagnostic ions with sufficient specificity (> 80%) for the bi-sialylated *N*-glycan containing a combination of α2,3 and α2,6 sialic acid linkages (Fig. 6c) were not able to be identified most likely due to the

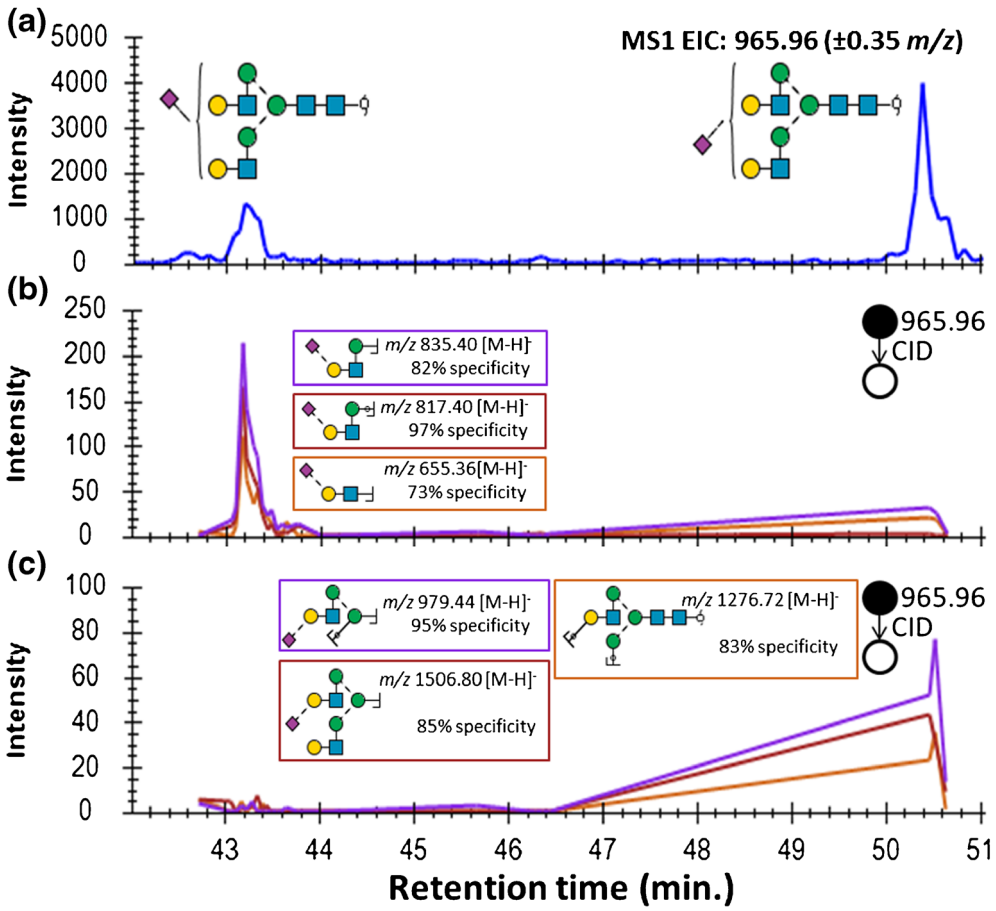

Figure 5. Automated mono-sialylated *N*-glycan sialyl-isomer discrimination using candidate diagnostic product ions. EICs of (**a**) the glycan precursor (*m/z* 965.96 $[M\text{-}2H]^{2-}$ $(Man)_3(Gal)_2(GlcNAc)_4(NeuAc)_1$), (**b**) the previously unreported diagnostic ions for α2,6-sialic acid linkage, and (**c**) the previously unreported diagnostic ions for α2,3-sialic acid linkage isomer

mixture of linkages, with each sialic acid linkage also represented in at least one other isomer.

Unlike the diagnostic ions for the arm position and singly sialylated glycan isomers covered earlier in this manuscript, the most specific fragments for the bi-sialylated bi-antennary *N*-glycans were all the result of multiple cleavages including a cross-ring cleavage. Although these cross-ring cleavage products are not theoretically specific for one glycan isomer, they were still more specific than other fragments generated by glycosidic bond cleavage alone. The ability to produce MS/MS spectra containing product ions resulting from all forms of glycan cleavage demonstrates the versatility of negative mode MS/MS for glycan isomer discrimination.

Discrimination of Sialyl Linkages by Specific Fragment Ions: O-Glycans

O-glycans are a less frequently studied area, despite their importance in breast and colon cancers [31]. Similar to *N*-glycans, *O*-glycans lack a panel of reported and validated diagnostic ions resulting from glycosidic bond cleavage for discrimination of glycan isomers featuring α2,3 sialic acid linkages. As shown in Fig. 7, using the candidate diagnostic ions for α2,6-sialyl linkage (*m/z* 615.32 ($^{1,3}X_{1\alpha}$), 513.24 ($Y_{1\alpha}$) and α2,3-sialic acid linkage (*m/z* 631.32 ($^{1,3}X_2$), 204.08 (Z_1)), we have identified glycosidic and cross-ring cleavage product ions specific (> 95%) for the different mono-sialylated *O*-glycans. Similar to the mono-sialylated bi-antennary *N*-glycan isomers, we were unable to detect previously published [18] discriminatory ions (*m/z* 512.20 ($^{2,4}A_3$), 306.1 ($^{0,4}A_2\text{-}CO_2$)) and/or they were at lower abundance and less specific (*m/z* 470.20 (C_2)) than the product ions identified in our study. This further confirms our hypothesis that the method of CID fragmentation can be important since the standard, sialyllactosamine, used for identifying diagnostic ions in the previous study, which used beam-type CID, is structurally similar to the sialylated *O*-glycans.

Assessment of Specificity for Isomer Discrimination

The usefulness of the candidate product ions as diagnostic ions, commonly assessed by comparing MS/MS spectra, does not provide an assessment of their specificity for isomer discrimination on a chromatographic time scale. Our method has its limitations in effectively quantitatively assessing specificity, namely because it was a data-dependent acquisition (DDA) experiment, rather than a selected reaction monitoring (SRM)

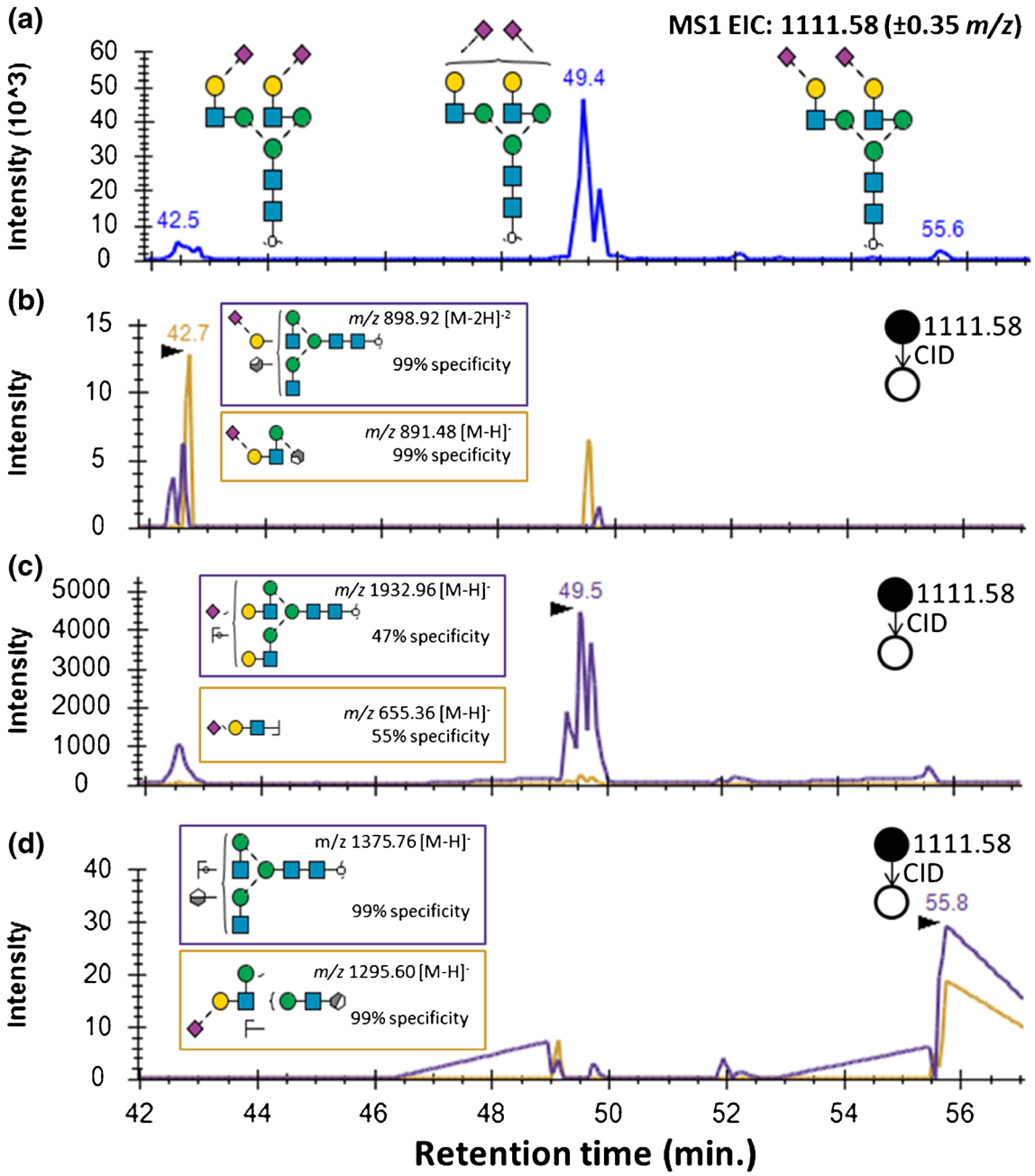

Figure 6. Automated bi-sialylated *N*-glycan sialic acid linkage isomer discrimination using candidate diagnostic product ions. EICs of (**a**) the glycan precursor (*m/z* 1111.58 $[M\text{-}2H]^{2-}$ $(Man)_3(Gal)_2(GlcNAc)_4(NeuAc)_2$). (**b**) The previously unreported diagnostic ions for α2,6-/α2,6-sialic acid linkage isomer, (**c**) the most specific ions for α2,3-/α2,6-sialic acid linkage isomer, and (**d**) the previously unreported diagnostic ions for α2,3/α2,3-sialic acid linkage isomer

or multiple reaction monitoring (MRM) experiment. Despite this, our assessment of specificity is more applicable and relatable to shotgun glycomics experiments.

Our measure of specificity was also very useful for understanding the effect of collision energy on specificity of the generation of candidate diagnostic ions. In Supp. Fig. 1, the specificity of candidate discriminatory ions for 3-arm and 6-arm extension was assessed. With varying collision energies, the specificity of these candidates was found to vary from 70 to 100% with 38% NCE providing, overall, the best specificities for isomer discrimination. Similar to the discriminants for 3-arm and 6-arm position, varying collision energies resulted in specificities ranging from 65 to 100%, and 33% NCE was found to provide, overall, the best specificities for sialic acid linkage isomer discrimination. Similarly to the determination of the arm position (Fig. 3), 48% NCE resulted in the lowest specificity of the identified diagnostic ions, again highlighting the importance of fragmentation energy optimization in

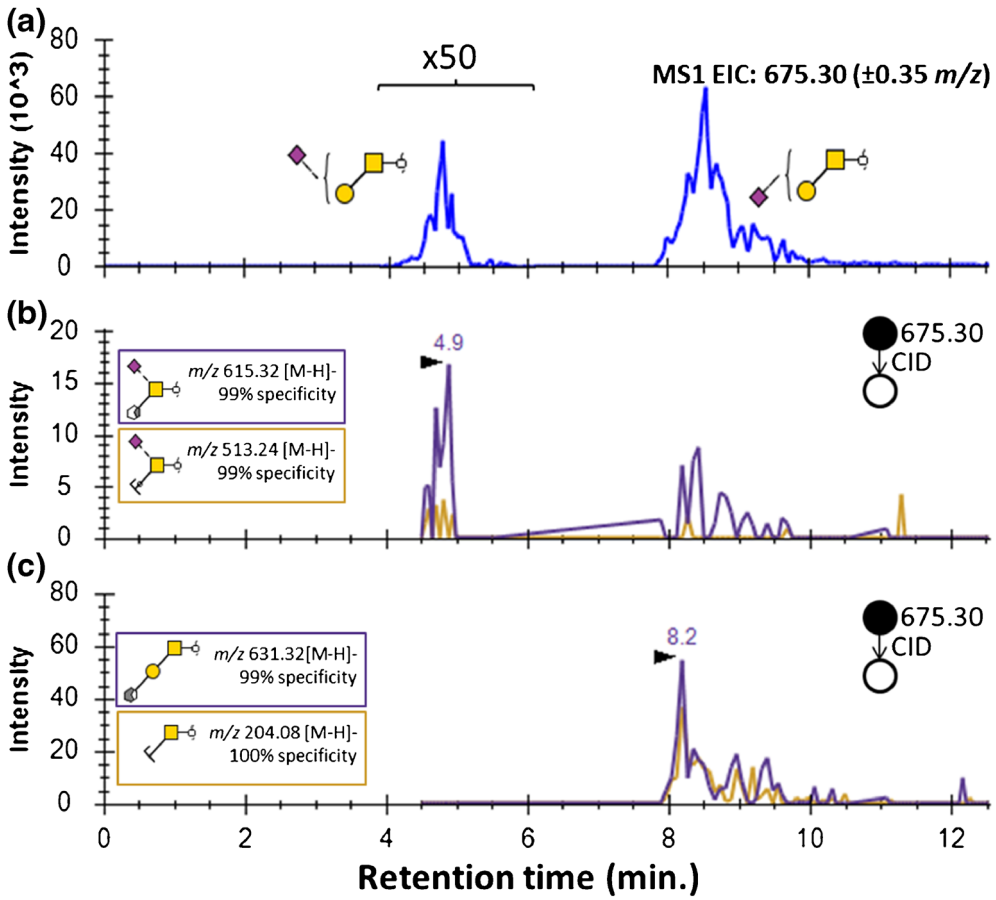

Figure 7. Automated mono-sialylated *O*-glycan sialic acid linkage isomer discrimination using candidate diagnostic product ions. EICs of (**a**) the glycan precursor (*m/z* 675.30 $[M\text{-}H]^{1-}$ $(Gal)_1(GalNAc)_1(NeuAc)_1$). (**b**) The previously unreported diagnostic ions for α2,6-sialic acid linkage isomer and (**c**) the previously unreported diagnostic ions for α2,3-sialic acid linkage isomer

distinguishing glycan isomers. Through this optimization of collision energy, we have determined the best structurally diagnostic ions in a platform able to be used for automated glycan isomer discrimination.

Another finding of interest was for the sialic acid linkage and arm position structural features represented by the diagnostic product ions were not theoretically specific (in silico fragmentation of glycan structure) for their respective isomers (e.g., cross-ring cleavage theoretically specific for one isomer over the other, as utilized by Yu et al. [32]). This is contrasted by the theoretically specific core-fucose diagnostic ion (*m/z* 368.23 ($Y_{1\alpha}$)) used in the structural characterization of the core-fucosylated glycan in Fig. 1. Our hypothesis is that slight differences in the overall glycan structure can result in certain dissociation pathways being favored by one glycan structural isomer over another. Research aiming to understand the fundamental theory of the role of glycan structure on the dissociation pathway has recently become an area of increased focus and could provide more insight into generation of these product ions diagnostic for certain structural features [33].

As demonstrated, we were able to identify diagnostic ions specific for arm position of bi-antennary *N*-glycans and sialic acid linkages of *N*- and *O*-glycans. One key question that remains is the robustness of these diagnostic ions: do these ions remain isomer specific in sample preparation replicates and on other ion trap platforms?

Assessment the Robustness of Diagnostic Fragments

The identification of diagnostic product ions often has not been incorporated into downstream automated software applications, leaving the characterization of glycans with these diagnostic ions to be largely manual and therefore tedious and somewhat subjective. Identification of these diagnostic ions in this study involved post-acquisition manual identification of fragments. For these diagnostic ions to be utilized more widely, fragmentation must be consistent beyond the sample and the instrument platform.

The diagnostic ions for specific arm extension on bi-antennary *N*-glycans were assessed in their use by sample replicates and analyses on other ion trap platforms (Fig. 8). For a sample preparation technical duplicate on the same platform, correct peak picking was successful, demonstrating that these ions are frequently observed and therefore remain useful diagnostics in replicate samples. When that same sample was

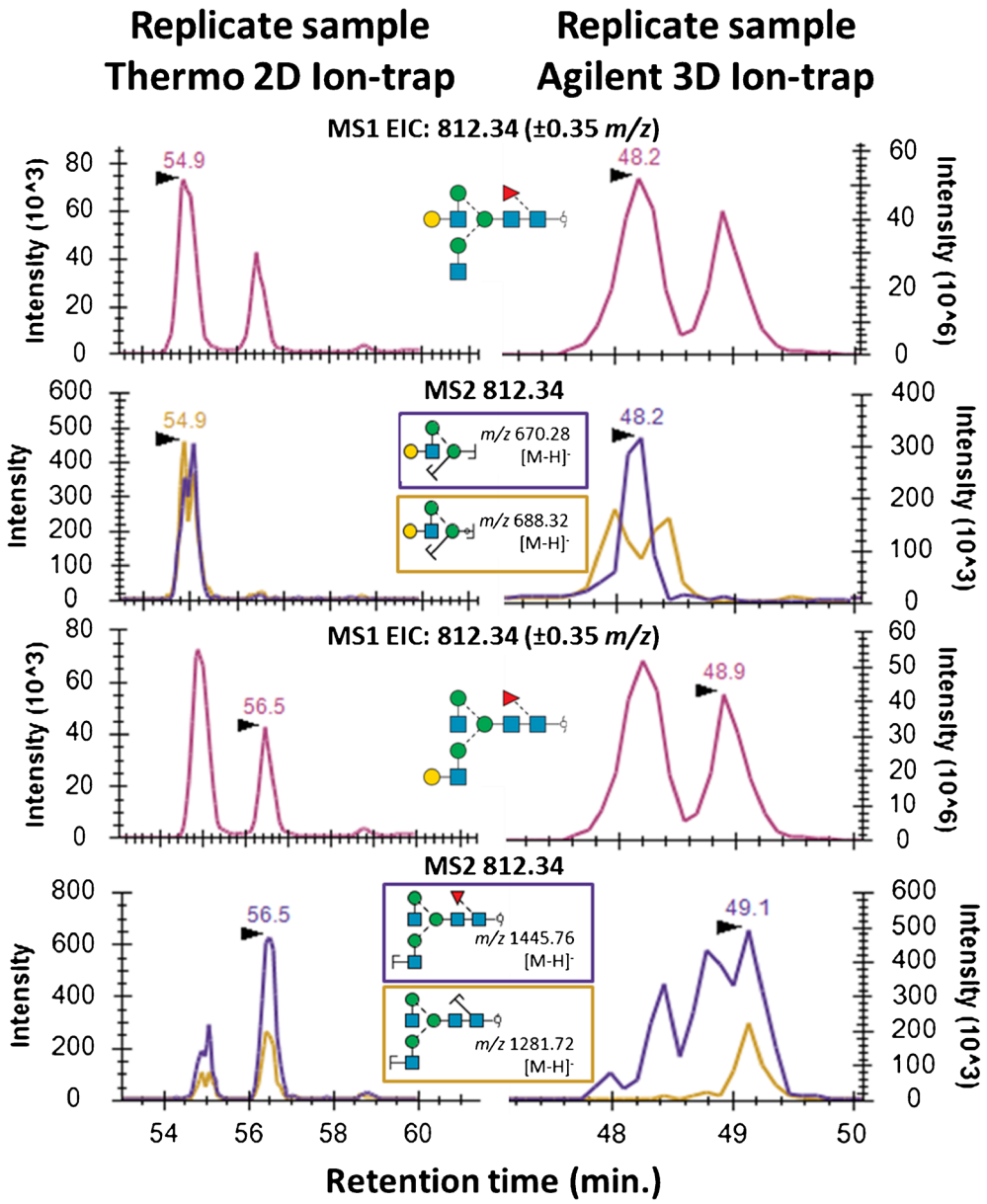

Figure 8. Application of diagnostic product ions for automated peak picking of *N*-glycan 3- and 6-arm composition isomers from technical replicate samples and independent LC-MS platforms. On the left, sample preparation replicate run on the Thermo linear ion trap and on the right, sample preparation replicate run

analyzed on a 3D ion trap, as opposed to the linear ion trap used for identifying these diagnostic product ions, integration of the correct peak was again successful. As shown in Supp. Figs. 4 and 5, this also applies to the other glycans (mono-sialylated *N*- and *O*-glycans) for which diagnostic ions were identified. Mono-sialylated *N*-glycan and *O*-glycan isomers were able to be discriminated using the identified diagnostic ions in both technical replicate samples and on both ion trap platforms.

We found this interesting as the two ion trap platforms feature different instrument architecture (linear vs. 3D) and each platform utilizes vendor-specific parameters for fragmentation (ramping voltage on Bruker and flat NCE for Thermo). Discriminatory ions appeared to be of similar, if not increased, specificity on the 3D ion trap platform demonstrating that these ions are still discriminatory despite optimization of collision energy not being performed on this platform.

As this approach is highly dependent on glycan structure and charge state, small structural changes could result in product ion specificity changes. To investigate if this was the case for sialic acid linkage determination, and see if our methods are applicable to a complex mixture such as a cell lysate, we used diagnostic ions for the mono-sialylated bi-antennary *N*-glycan (Fig. 5) and applied it to core-fucosylated mono-sialylated bi-antennary *N*-glycan isomers (Supp. Fig. 6) released from glycoproteins of a J774 cell lysate. Two of the diagnostic ions previously used were not suitable for these closely related

structures, with one of the ions (*m/z* 835.40, used for discriminating the α2,6 sialic acid linkage) non-specific and the other ion (*m/z* 979.44, used for discriminating the α2,3 sialic acid linkage) not detected in the MS/MS spectra from either isomer. The remaining diagnostic ions (*m/z* 817.40 (B_4), 655.36 (B_3), 1276.72 ($Y_{6\beta}Y_{4\alpha}$), and 1506.80 (B_5)), established for the mono-sialylated *N*-glycan isomers, remained effective for discriminating between the core-fucosylated mono-sialylated *N*-glycan isomers, with surprisingly increased specificity.

This observation could be explained by the fact that the specific diagnostic ions used for discrimination of sialic acid linkages are B- and C-type fragment ions for the α2,6-sialyl linkage isomer and Y-/B- and B-type fragment ions for the α2,3-sialyl linkage isomer; the chitobiose core, where the fucose is attached, is not featured in these cleavage products. The majority of these product ions are however specific for both core-fucosylated and non-core-fucosylated forms of mono-sialylated bi-antennary *N*-glycans, such that identification and validation of candidate discriminatory ions can be performed for each of these glycan isomer types.

For this study, at least two specific product ions per isomer were identified. We have observed that using more than one diagnostic ion for glycan isomer discrimination increases the specificity and thus confidence in characterizing the correct glycan isomer. In the case of more than one structural feature differing between glycan isomers, the use of additional diagnostic ions for each feature could be of benefit.

As automated discrimination of these glycan isomers was performed using instrument platforms set up for discovery-focused shotgun glycomics, this discrimination is compatible with ion trap-based shotgun glycomics experiments, removing the need for targeted pseudo-MS3 analysis ([34]) which has been demonstrated to discriminate similar glycan isomers. To improve the robustness and reproducibility of this workflow for automated glycan isomer analysis, orthogonal data collected from the same run (such as PGC retention time) can also be used to validate the isomer identification [3]. We have also found this method is also compatible with at least one other form of CID, beam-type higher-energy collisional dissociation (HCD). Analyzing the same glycan mixtures with ion trap HCD as the fragmentation method, we have found similar specificities (67–100%) for almost all of the identified product ions (with one exception) to discriminate arm composition and sialylation (Sup Fig. 7).

The Skyline platform was used for assessing specificity and automated peak picking using the identified diagnostic ions, as this software is able to be used with data generated from different vendors and a wide range of mass analyzers. This identifies it as useful software which can be used to implement these fragmentation discriminators for automated glycan isomer discrimination. The use of MS/MS filtering in Skyline with a targeted filtering method was used in this case, although a targeted acquisition method was not used. Unlike previous uses of Skyline for glycomics [35], retention time filtering was not used and was not required for correct peak picking. We see this as a benefit as the use of explicit retention times, in combination with glycan mass, to define glycan structural isomers can lead to erroneous or missed glycan structure quantitation, as column age can result in altered elution characteristics on a porous graphitized carbon stationary phase [36]. The use of an internal retention time standard, such as dextran, could be used for retention time realignment [37] but this has not been accomplished for non-derivatized label-free glycan analysis.

Many of the previous publications identifying diagnostic ions for glycan structure determination have not had the benefit of data repositories or a place for making chromatograms easily accessible. However, from this publication, all data files and Skyline assays used for the automated glycan isomer discrimination and specificity calculations are available on Panorama [38] (https://panoramaweb.org/labkey/project/home/begin.view?) and Chorus [39] (https://chorusproject.org/pages/index.html). This allows improved dissemination and application of these diagnostic ions in the glycomics analytical community.

Conclusion

Sialylation and arm position are biologically important glycan structural features generating closely related isomers that are difficult to confirm by MS/MS alone. We here report a workflow to identify product ions that can identify these structural features and discriminate sialyl linkage on both *N*- and *O*-glycans and arm position on *N*-glycan isomers. These product ions are structure-specific and can also be substructure specific, in the case of the sialic acid linkage on mono-sialylated *N*-glycans with and without core-fucose. While these diagnostic ions have only been identified for native reduced glycans analyzed in negative mode, this workflow has the potential to be used for identification of diagnostic ions for alternative mass spectrometry-based glycan analysis methods such as derivatized glycans or analysis in positive ion mode.

The Skyline software was used to quantify the specificity of these diagnostic ions and implement them into automated glycan isomer integration. These diagnostic ions were robust enough to discriminate between glycan isomers in a complex mixture and were successfully used to interpret data from both linear and 3D ion traps. This workflow may be able to be extended to other glycan isomers that are currently challenging to discriminate based on MS/MS alone.

Acknowledgements

This study was supported by an Australian Postgraduate Award scholarship. We thank M. P. C., Griffith University, for the useful discussions. We also thank the Skyline development team for creating and developing the Skyline software package. This research project was facilitated by access to the Australian Proteomics Analysis Facility (APAF) established under the Australian Government's NCRIS program. C. A. is funded by an Australian Postgraduate Award. M.T.-A. was supported by a fellowship from the Cancer Institute NSW, Australia.

References

1. Lin, S., Kemmner, W., Grigull, S., Schlag, P.M.: Cell surface a2,6-sialylation affects adhesion of breast carcinoma cells. Exp. Cell Res. **110**, 101–110 (2002)
2. Zaia, J.: Mass spectrometry of oligosaccharides. Mass Spectrom. Rev. **23**, 161–227 (2004)
3. Abrahams, J.L., Campbell, M.P., Packer, N.H.: Building a PGC-LC-MS N-glycan retention library and elution mapping resource. Glycoconj. J. 1–15 Advance online publication. https://doi.org/10.1007/s10719-017-9793-4. (2017)
4. Pabst, M., Bondili, J.S., Stadlmann, J., Mach, L., Altmann, F.: Mass + retention time = structure: a strategy for the analysis of N-glycans by carbon LC-ESI-MS and its application to fibrin N-glycans. Anal. Chem. **79**, 5051–5057 (2007)
5. Harvey, D.J.: Fragmentation of negative ions from carbohydrates: part 1. Use of nitrate and other anionic adducts for the production of negative ion electrospray spectra from N-linked carbohydrates. J. Am. Soc. Mass Spectrom. **16**, 622–630 (2005)
6. Harvey, D.J.: Fragmentation of negative ions from carbohydrates: part 2. Fragmentation of high-mannose N-linked glycans. J. Am. Soc. Mass Spectrom. **16**, 631–646 (2005)
7. Harvey, D.J.: Fragmentation of negative ions from carbohydrates: part 3. Fragmentation of hybrid and complex N-linked glycans. J. Am. Soc. Mass Spectrom. **16**, 647–659 (2005)
8. Harvey, D.J., Jaeken, J., Butler, M., Armitage, A.J., Rudd, P., Dwek, R.A.: Fragmentation of negative ions from N-linked carbohydrates, part 4. Fragmentation of complex glycans lacking substitution on the 6-antenna. J. Mass Spectrom. **45**, 528–535 (2010)
9. Harvey, D.J., Rudd, P.M.: Fragmentation of negative ions from N-linked carbohydrates. Part 5: anionic N-linked glycans. Int. J. Mass Spectrom. **305**, 120–130 (2011)
10. Harvey, D.J., Edgeworth, M., Krishna, B.A., Bonomelli, C., Allman, S.A., Crispin, M., Scrivens, J.H.: Fragmentation of negative ions from N-linked carbohydrates: part 6. Glycans containing one N-acetylglucosamine in the core. Rapid Commun. Mass Spectrom. **28**, 2008–2018 (2014)
11. Harvey, D.J., Abrahams, J.L.: Fragmentation and ion mobility properties of negative ions from N-linked carbohydrates: part 7. Reduced glycans. Rapid Commun. Mass Spectrom. **30**, 627–634 (2016)
12. Pfenninger, A., Karas, M., Finke, B., Stahl, B.: Structural analysis of underivatized neutral human milk oligosaccharides in the negative ion mode by nano-electrospray MSn (part 1: methodology). J. Am. Soc. Mass Spectrom. **13**, 1331–1340 (2002)
13. Doohan, R.A., Hayes, C.A., Harhen, B., Karlsson, N.G.: Negative ion CID fragmentation of o-linked oligosaccharide aldoses-charge induced and charge remote fragmentation. J. Am. Soc. Mass Spectrom. **22**, 1052–1062 (2011)
14. Harvey, D.J., Martin, R.L., Jackson, K.A., Sutton, C.W.: Fragmentation of N-linked glycans with a matrix-assisted laser desorption/ionization ion trap time-of-flight mass spectrometer. Rapid Commun. Mass Spectrom. **18**, 2997–3007 (2004)
15. Bereman, M.S., Canterbury, J.D., Egertson, J.D., Horner, J., Remes, P.M., Schwartz, J.C., Zabrouskov, V., Maccoss, M.J.: Evaluation of front-end higher energy collision-induced dissociation on a bench-top dual pressure linear ion trap mass spectrometer for shotgun proteomics. Anal. Chem. **84**, 1533–1539 (2012)
16. Domon, B., Costello, C.E.: A systematic nomenclature for carbohydrate fragmentations in FAB-MS/MS spectra of glycoconjugates. Glycoconj. J. **5**, 397–409 (1988)
17. Everest-Dass, A.V., Abrahams, J.L., Kolarich, D., Packer, N.H., Campbell, M.P.: Structural feature ions for distinguishing N- and O-linked glycan isomers by LC-ESI-IT MS/MS. J. Am. Soc. Mass Spectrom. **24**, 895–906 (2013)
18. Wheeler, S.F., Harvey, D.J.: Negative ion mass spectrometry of sialylated carbohydrates: discrimination of N-acetylneuraminic acid linkages by MALDI-TOF and ESI-TOF mass spectrometry. Anal. Chem. **72**, 5027–5039 (2000)
19. Spina, L., Romeo, D., Impallomeni, G., Garozzo, D., Waidelich, D., Glueckmann, M.: New fragmentation mechanisms in matrix-assisted laser desorption/ionization time-of-flight/time-of-flight tandem mass spectrometry of carbohydrates. Rapid Commun. Mass Spectrom. **18**, 392–398 (2004)
20. Ranzinger, R., Weatherly, D., Arpinar, S., Khan, S., Porterfield, M., Tiemeyer, M., S. W. York: GRITS Toolbox—a software system for the archival, processing and interpretation of glycomics data. In: Annual Meeting of the Society-for-Glycobiology on Glycobiology. p. 1275 (2015)
21. Yu, C.Y., Mayampurath, A., Hu, Y., Zhou, S., Mechref, Y., Tang, H.: Automated annotation and quantification of glycans using liquid chromatography-mass spectrometry. Bioinformatics. **29**, 1706–1707 (2013)
22. MacLean, B., Tomazela, D.M., Shulman, N., Chambers, M., Finney, G.L., Frewen, B., Kern, R., Tabb, D.L., Liebler, D.C., MacCoss, M.J.: Skyline: an open source document editor for creating and analyzing targeted proteomics experiments. Bioinformatics. **26**, 966–968 (2010)
23. Bradford, M.M.: A rapid and sensitive method for the quantitation of microgram quantities of protein utilizing the principle of protein-dye binding. Anal. Biochem. **72**, 248–254 (1976)
24. Jensen, P.H., Karlsson, N.G., Kolarich, D., Packer, N.H.: Structural analysis of N- and O-glycans released from glycoproteins. Nat. Protoc. **7**, 1299–1310 (2012)
25. Kessner, D., Chambers, M., Burke, R., Agus, D., Mallick, P.: ProteoWizard: open source software for rapid proteomics tools development. Bioinformatics. **24**, 2534–2536 (2008)
26. Nagy, G., Pohl, N.L.B.: Monosaccharide identification as a first step toward de novo carbohydrate sequencing: mass spectrometry strategy for the identification and differentiation of diastereomeric and enantiomeric pentose isomers. Anal. Chem. **87**, 4566–4571 (2015)
27. Webb, I.K., Chen, T.C., Danielson, W.F., Ibrahim, Y.M., Tang, K., Anderson, G.A., Smith, R.D.: Implementation of dipolar resonant excitation for collision induced dissociation with ion mobility/time-of-flight MS. J. Am. Soc. Mass Spectrom. **25**, 563–571 (2014)
28. Everest-Dass, A.V., Jin, D., Thaysen-Andersen, M., Nevalainen, H., Kolarich, D., Packer, N.H.: Comparative structural analysis of the glycosylation of salivary and buccal cell proteins: innate protection against infection by Candida albicans. Glycobiology. **22**, 1465–1479 (2012)
29. Harvey, D.J., Royle, L., Radcliffe, C.M., Rudd, P.M., Dwek, R.A.: Structural and quantitative analysis of N-linked glycans by matrix-assisted laser desorption ionization and negative ion nanospray mass spectrometry. Anal. Biochem. **376**, 44–60 (2008)
30. Mcclellan, J.E., Costello, C.E., Connor, P.B.O., Zaia, J.: Influence of charge state on product ion mass spectra and the determination of 4S / 6S sulfation sequence of chondroitin sulfate oligosaccharides. Anal. Chem. **74**, 3760–3771 (2002)
31. Brockhausen, I.: Mucin-type O-glycans in human colon and breast cancer: glycodynamics and functions. EMBO Rep. **7**, 599–604 (2006)
32. Yu, X., Huang, Y., Lin, C., Costello, C.E.: Energy-dependent electron activated dissociation of metal-adducted permethylated oligosaccharides. Anal. Chem. **84**, 7487–7494 (2012)
33. Bythell, B.J., Abutokaikah, M.T., Wagoner, A.R., Guan, S., Rabus, J.M.: Cationized carbohydrate gas-phase fragmentation chemistry. J. Am. Soc. Mass Spectrom. **28**, 688–703 (2017)
34. Chen, C.-H., Lin, Y.-P., Lin, J.-L., Li, S.-T., Ren, C.-T., Wu, C.-Y., Chen, C.-H.: Rapid identification of terminal sialic acid linkage isomers by pseudo-MS3 mass spectrometry. Isr. J. Chem. **55**, 412–422 (2015)
35. Loziuk, P.L., Hecht, E.S., Muddiman, D.C.: N-linked glycosite profiling and use of Skyline as a platform for characterization and relative quantification of glycans in differentiating xylem of *Populus trichocarpa*. Anal. Bioanal. Chem. **409**, 487–497 (2017)
36. Pabst, M., Altmann, F.: Influence of electrosorption, solvent, temperature, and ion polarity on the performance of LC-ESI-MS using graphitic carbon for acidic oligosaccharides. Anal. Chem. **80**, 7534–7542 (2008)
37. Guile, G.R., Rudd, P.M., Wing, D.R., Prime, S.B., Dwek, R.A.: A rapid high-resolution high-performance liquid chromatographic method for separating glycan mixtures and analyzing oligosaccharide profiles. Anal. Biochem. **240**, 210–226 (1996)
38. Sharma, V., Eckels, J., Taylor, G.K., Shulman, N.J., Stergachis, A.B., Joyner, S.A., Yan, P., Whiteaker, J.R., Halusa, G.N., Schilling, B., Gibson, B.W., Colangelo, C.M., Paulovich, A.G., Carr, S.A., Jaffe, J.D., Maccoss, M.J., Maclean, B.: Panorama: a targeted proteomics knowledge base. J. Proteome Res. **13**, 4205–4210 (2014)
39. Loo, J.A., Matthews, D.E., Yates, J.R.: Focus on bioinformatics, software, and MS-based "Omics," honoring Dr. Michael J. MacCoss, recipient of the 2015 ASMS Biemann medal. J. Am. Soc. Mass Spectrom. **27**, 1715–1718 (2016)

40. Kolarich, D., Rapp, E., Struwe, W.B., Haslam, S.M., Zaia, J., McBride, R., Agravat, S., Campbell, M.P., Kato, M., Ranzinger, R., Kettner, C., York, W.S.: The minimum information required for a glycomics experiment (MIRAGE) project: improving the standards for reporting mass-spectrometry-based glycoanalytic data. Mol. Cell. Proteomics. **12**, 991–995 (2013)